Signal Processing 208 (2023) 108958

Contents lists available at ScienceDirect

Signal Processing

journal homepage: www.elsevier.com/locate/sigpro

Kalman filter/smoother-based design and implementation of digital IIR filters

Arman Kheirati Roonizi [a,b]

[a] Dipartimento di Informatica, Università degli Studi di Milano, Via Celoria 18, Milano 20131, Italy
[b] Department of Computer Science, Fasa University, Daneshjou blvd, Fasa 74616-86131, Iran

ARTICLE INFO

Article history:
Received 29 November 2021
Revised 29 January 2023
Accepted 1 February 2023
Available online 5 February 2023

Keywords:
Digital IIR filter
Kalman filter
Kalman smoother
Wiener filter
Optimization

ABSTRACT

Recently, a unified framework was proposed for forward-backward filtering and penalized least-squares optimization. It was shown that forward-backward filtering can be presented as instances of penalized least-squares optimization. In other words, the output of a zero-phase digital infinite-impulse response (IIR) filter can be computed by solving a constrained optimization problem, in which the weight controlling the constraint is directly related to cutoff frequencies with closed-form equations. It was also shown that a zero-phase digital IIR filter can be formed as an optimal smoothing Wiener filter for a random process obtained from an autoregressive (AR) or AR-moving average (ARMA) model driven by input (innovation) noise in presence of an observation noise.

In this paper, the problem of zero-phase digital IIR filtering is re-examined using Kalman filter/smoother. The paper shows that every zero-phase digital IIR filter can be viewed as a special case of an optimal smoothing Wiener filter. Based on the fact that the formulations of the optimum filter by Wiener and Kalman are equivalent in steady state, we present a Kalman filter/smoother framework to the design and implementation of digital IIR filters. As an example, the zero-phase digital Butterworth filter is designed using Kalman smoother and compared with the traditional design (forward filtering and backward smoothing) method.

1. Introduction

1.1. Digital IIR filter

Linear time invariant (LTI) filters play a significant role in the development of various signal processing techniques [13,23]. The main advantage of LTI filters is their inherent simplicity. Design, analysis, and implementation of such filters are relatively straightforward tasks in many applications. The properties of LTI filters are well understood, and many effective methods exist for their design and efficient implementation. A digital filter can be described as various equivalent formulations, e.g., the transfer function formulation, difference equation formulation, and state space formulation. Many papers and a lot of books have appeared (see Oppenheim and Schafer [13], Parks and Burrus [14], Smith [23] and the references therein). The basic approach relies on the fact that an LTI system can be characterized by its impulse response, which is defined as the output response to an impulse input [13]. It is well known that the output signal of an LTI system is obtained by the convolution of the input signal with the system's impulse response. In this technique, the desired filter is first designed in the frequency domain (e.g., minimax design of IIR digital filters [1,11,17]) and then implemented in the time domain using convolution operator (the convolution in the time domain is equivalent to multiplication in the frequency or z-transform domain). A similar approach is based on the Fourier transform. It involves transforming the signal into the frequency domain, using a fast Fourier transform (FFT), applying the filter as a frequency-wise multiplication, and computing an inverse Fourier transform to obtain the filtered signal. Therefore, there is a need for an additional "inverse transform" step to find the time-domain signal, which could be quite involved. That is why the problem of finding the impulse response of an LTI system directly in time domain has attracted the researchers. A closed-form expression has been developed by Shahrrava to find the impulse response by introducing an additional difference equation according to the LTI system [20]. Shahrrava's approach is suitable for finding the impulse response of LTI systems. However, the output signal, which is of interest in practice, has to be computed through the convolution of the impulse response with the input signal, at additional cost. Liu and Pei extended Shahrrava's approach and presented a time-domain approach to find the closed-form output response of discrete-time LTI systems [12]. In other approaches, the output of digital IIR filters are computed using a state-space formulation with an initial condition [16,23].

E-mail addresses: a-kheirati@fasau.ac.ir, arman.kheirati@unimi.it

https://doi.org/10.1016/j.sigpro.2023.108958

More recent and effective approaches handle the problem of digital IIR smoothing filter design, directly in time domain, by defining (or solving) a constraint least-squares optimization problem [3,8–10]. These approaches are based on the fact that a zero-phase digital IIR filter can be formed as an optimal smoothing Wiener filter for a random process obtained from an AR/ARMA model driven by input white (innovation) noise in presence of white or colored observation noise. Then a zero-phase digital IIR filter is designed by solving an optimization problem with a smoothing constraint. In [10], a framework for unification of regularized least-squares optimization and forward-backward filtering scheme was presented. In [9], the problem of band-stop smoothing filter (BSSF) design is investigated directly in the time domain using a regularized least-squares optimization algorithm. It is shown that with the optimization approaches, the cutoff frequencies are related to the regularized parameters and the filter order can be directly (and easily) controlled with the number of derivatives. In [3], an efficient ARMA smoothing filter was proposed. The efficiency stems from the use of an optimization algorithm to solve the smoothing/denoising problem directly in the time domain. The method is defined as the problem of minimizing the ℓ_2-norm of the ARMA model error subject to a data fidelity constraint. Recently, a Kalman filter/smoother framework was introduced in Kheirati Roonizi [5] to the design and implementation of ℓ_2 and ℓ_1 trend filtering.

The current paper attempts to give a Kalman filter/smoother formulation for the design and implementation of digital IIR filters. Based on the fact that a zero-phase digital IIR filter can be viewed as an optimal smoothing Wiener filter, a Kalman filter/smoother framework is proposed to estimate the output response of (zero-phase) digital IIR filters.

The rest of the paper is as follows. Some basic concepts of Wiener and Kalman filter theory are presented in the following section. Section 2 describes the problem and issue that we seek to address in this paper. In Section 3, a Kalman filter or smoother is proposed to compute the output response of digital IIR filters. Some examples are given in Section 4. We use the proposed theory for implementing the zero-phase digital Butterworth filters. In Section 5, we compare the proposed approach and the traditional convolutional approach based output computation of digital Butterworth filter for denoising the photoplethysmography (PPG) signals. Some general remarks and future direction are given in the final section.

1.2. Wiener and Kalman filter theory

The Kalman filter is one of the major contributions of Rudolf E. Kálmán [2] in the field of information processing, an optimal estimator in the minimum mean-square error (MMSE) sense for estimating the hidden state of a linear dynamical system [22]. Before Kalman, Nobert Wiener introduced the first theory in merging the dynamic systems and optimal estimation in the presence of noise (i.e., Wiener filter) [25]. The task of Wiener filter is to produce an optimal estimate of a random signal using both the autocorrelation and crosscorrelation of the measurement signal with the original signal. It minimizes the MSE between the estimated random process and the desired process.

1.2.1. Wiener filter

Let s_k be a an unknown signal which must be estimated from a measurement signal y_k in the model:

$$y_k = \theta_k * s_k + \eta_k, \quad k = 1, \dots, L \tag{1}$$

where θ_k is an impulse response, η_k is the observation noise and $*$ denotes the convolution operator. As depicted in Fig. 1, the aim of filter design is to find a filter such that when the measurements

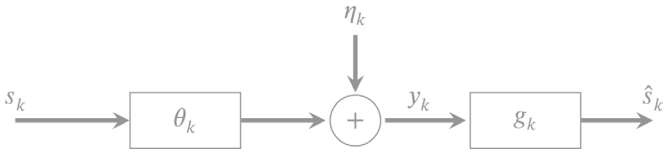

Fig. 1. Signal model for Wiener filter.

y_k pass through it, the filter output produces the MSE estimate of the signal of interest, s_k:

$$\hat{s}_k = g_k * y_k \approx s_k \tag{2}$$

where g_k is the filter impulse response and $\hat{s}_k$ is an estimate of the desired signal. To this aim, we define the error signal $e_k \triangleq s_k - \hat{s}_k$ and carry out the following minimization:

$$\underset{g_k}{\operatorname{argmin}}[\mathbb{E}\{e_k^2\} = r_{ee}(0)] = \underset{g_k}{\operatorname{argmin}}\mathbb{E}\{(s_k - g_k * y_k)^2\} \tag{3}$$

where $\mathbb{E}\{\}$ refers to the expected value operation and $r_{ee}(k)$ is the autocorrelation function (ACF) of e_k. If s_k and η_k are uncorrelated, the optimum Wiener filter is obtained by setting the derivative of (3) with respect of g_k to zero [15,25]:

$$G(z) = S_{\boldsymbol{ss}}(z)\theta(\frac{1}{z})\Big[\theta(z)S_{ss}(z)\theta(\frac{1}{z}) + S_{\eta\eta}(z)\Big]^{-1}, \tag{4}$$

where $G(z)$ and $\theta(z)$ are the Z-transform of g_k and θ_k, respectively, $S_{ss}(z)$ and $S_{\eta\eta}(z)$ are the spectra of s_k and η_k, respectively.

1.2.2. Kalman filter

Let us consider the following linear discrete dynamical system

$$\begin{cases} \boldsymbol{\xi}_k = \boldsymbol{\Phi}\boldsymbol{\xi}_{k-1} + \boldsymbol{\Sigma}\boldsymbol{w}_k \\ \boldsymbol{y}_k = \boldsymbol{H}\boldsymbol{\xi}_k + \boldsymbol{\eta}_k \end{cases}, \tag{5}$$

where $\boldsymbol{\xi}_k$ is the state vector containing the terms of interest for the system, $\boldsymbol{\Phi}$ is the state transition matrix of the process from the state at time $k-1$ to the state at time k and $\boldsymbol{w}_k$ is the process noise vector with known covariance, $\boldsymbol{Q}_k \triangleq \mathbb{E}\{\boldsymbol{w}_k^T\boldsymbol{w}_k\}$. $\boldsymbol{y}_k$ is the vector of observations, $\boldsymbol{H}$ is the transformation matrix which relates the state variables to the measurements and $\boldsymbol{\eta}_k$ is the vector containing the observation noise terms with known covariance, $\boldsymbol{R}_k \triangleq \mathbb{E}\{\boldsymbol{\eta}_k^T\boldsymbol{\eta}_k\}$. Kalman filter produces the optimal estimate of the state vector in the minimum mean square sense. It involves two stages: prediction and measurement updates:

Prediction Update:

$$\begin{cases} \hat{\boldsymbol{\xi}}_{k+1}^- = \boldsymbol{\Phi}_k\boldsymbol{\xi}_k^+ \\ \boldsymbol{P}_{k+1}^- = \boldsymbol{\Phi}_k\boldsymbol{P}_k^+\boldsymbol{\Phi}_k^T + \boldsymbol{\Sigma}^T\boldsymbol{Q}\boldsymbol{\Sigma} \end{cases}$$

Measurement update:

$$\begin{cases} \hat{\boldsymbol{\xi}}_k^+ = \hat{\boldsymbol{\xi}}_k^- + \boldsymbol{K}_k\Big[\boldsymbol{y}_k - \boldsymbol{H}\hat{\boldsymbol{\xi}}_k^-\Big] \\ \boldsymbol{K}_k = \boldsymbol{P}_k^-\boldsymbol{H}^T\big(\boldsymbol{h}\boldsymbol{P}_k\boldsymbol{H}^T + \boldsymbol{R}_k\big)^{-1} \\ \boldsymbol{P}_k^+ = \boldsymbol{P}_k^- - \boldsymbol{K}_k\boldsymbol{H}\boldsymbol{P}_k^- \end{cases}$$

where $\hat{\boldsymbol{\xi}}_k^- \triangleq \mathbb{E}\{\boldsymbol{\xi}_k|\boldsymbol{y}_{k-1}, \dots, \boldsymbol{y}_1\}$ is the *a priori* estimate of the state vector $\boldsymbol{\xi}_k$ in the kth stage using the observation $\boldsymbol{y}_1$ to $\boldsymbol{y}_{k-1}$, and $\hat{\boldsymbol{\xi}}_k^+ \triangleq \mathbb{E}\{\boldsymbol{\xi}_k|y_k, \dots, y_1\}$ is the *a posteriori* estimate of the state vector after using the kth observation $\boldsymbol{y}_k$. The matrices $\boldsymbol{P}_k^- \triangleq \mathrm{E}\{(\boldsymbol{\xi}_k - \hat{\boldsymbol{\xi}}_k^-)(\boldsymbol{\xi}_k - \hat{\boldsymbol{\xi}}_k^-)^T\}$ and $\boldsymbol{P}_k^+ \triangleq \mathrm{E}\{(\boldsymbol{\xi}_k - \hat{\boldsymbol{\xi}}_k^+)(\boldsymbol{\xi}_k - \hat{\boldsymbol{\xi}}_k^+)^T\}$ are also defined as the *prior* and *posterior* state covariance matrices, while $\boldsymbol{K}_k$ is the Kalman gain.

In order to perform smoothing, we simply need to rerun a Kalman filter in the backward direction and merge, for each k,

the information from the future with that of the past. Kalman smoother provides better estimates of the current states than Kalman filter in noisy scenarios as it uses information brought by "future" observations.

2. Problem definition

Let us consider a noisy measurement signal

$$y_k = x_k + \eta_k, \quad k = 1, \dots, L, \tag{6}$$

where x_k is the signal of interest and η_k is the unwanted noise signal. We assume that x_k is (approximately) restricted to a known frequency band and η_k can be modeled as

$$\eta_k = u_k + v_k, \tag{7}$$

where v_k is a white Gaussian noise and u_k is a band-limited signal. We further assume that the unwanted part, u_k, and the signal of interest, x_k, are on disjoint frequency ranges. The problem of estimating x_k in (6) or equivalently estimating and removing the noise, η_k, is required in many signal processing applications. Digital IIR filters are the most common approaches to eliminate the noise and reconstruct the signal of interest in (6).

An IIR filter with an input y_k and the output x_k^f can be represented in the form

$$\sum_{n=0}^{N} a_n x^f_{k-n} = \sum_{m=0}^{M} b_m y_{k-m}, \tag{8}$$

where a_n and b_m are the filter coefficients, and the output x_k^f is a linear combination of the previous N output samples $[x^f_{k-1}, \dots, x^f_{k-N}]$, the present input sample y_k and the previous M input samples $[y_{k-1}, \dots, y_{k-M}]$. Without loss of generality, the term a_0 in (8) is set equal to 1. The role of a digital IIR filter (8) is to pass the frequency band of x_k and reject other frequency band components. In other word, (8) is suitable for applications where the desired signal and the undesired signal are separable in frequency spectrum (i.e., x_k and u_k). However, the problem is that in many applications, the undesired signal may also contain a white Gaussian process (i.e., v_k) which has a uniform spectrum (flat power spectra). Therefore, the digital IIR filters fail to reject the white Gaussian noise. This shortcoming is due to the traditional design methods for finding the output response of digital IIR filters (i.e., the convolution methods). To overcome this problem, we derive a dynamical model for the output response of digital IIR filters such that the Kalman filter can be applied. In the first attempt, we derive a dynamical model for the desired signal based on the output response of digital IIR filters (i.e., x_k) and consider other parts ($\eta_k = u_k + v_k$) as observation noise. Kalman filter assumes that the observation noise is white Gaussian. In the second attempt, the model of u_k is also considered in parallel with the model of x_k. In this case, x_k and u_k are simultaneously tracked through Kalman filter and the only observation noise is v_k. Since v_k is a white Gaussian noise, the Kalman filter is optimal.

3. Digital IIR filter design using Kalman filter/smoother

Noting that x_{k-n} in time domain corresponds to $z^{-n}X(z)$ in z-domain, (8) can be represented in the frequency domain as

$$\begin{aligned} &X^f(z) = H(z)Y(z), \quad H(z) = \tfrac{B(z)}{A(z)} \\ &B(z) = \textstyle\sum_{m=0}^{M} b_m z^{-m}, \quad A(z) = \sum_{n=0}^{N} a_n z^{-n} \end{aligned}. \tag{9}$$

Note that an LTI system described by (8) is causal if $N \geq M$ and noncausal if $N < M$ [20]. We assume without loss of generality that $N \geq M$, unless otherwise stated. For notational convenience, in the following, we define $B(z)$ in (9) as

$$B(z) = \sum_{n=0}^{N} b_n z^{-n}, \tag{10}$$

where the value of b_n which is not defined in (9) is considered to be zero (i.e., $b_n = 0$, for $M < n \leq N$). A zero-phase digital IIR filter can be obtained by multiplying $H(z)$ with its conjugate:

$$G(z) = H(z)H(z^{-1}) = \frac{B(z)B(z^{-1})}{A(z)A(z^{-1})}. \tag{11}$$

It can be verified that [18]

$$\begin{cases} B(z)B(z^{-1}) = \displaystyle\sum_{n=-N}^{N} c_n z^{-n} \\ A(z)A(z^{-1}) = \displaystyle\sum_{n=-N}^{N} d_n z^{-n} \end{cases}, \tag{12}$$

where

$$\begin{cases} c_n = c_{-n} = \displaystyle\sum_{i=0}^{N-n} b_i b_{i+n}, \quad n = 0,\ 1, \dots, N \\ d_n = d_{-n} = \displaystyle\sum_{i=0}^{N-n} a_i a_{i+n}, \quad n = 0,\ 1, \dots, N \end{cases}.$$

We rewrite (11) as

$$G(z) = \frac{B(z)B(z^{-1})}{B(z)B(z^{-1}) + [A(z)A(z^{-1}) - B(z)B(z^{-1})]}, \tag{13}$$

which can be written again as

$$G(z) = \frac{B(z)B(z^{-1})}{B(z)B(z^{-1}) + \Upsilon(z)\Upsilon(z^{-1})}, \tag{14}$$

where

$$\Upsilon(z)\Upsilon(z^{-1}) = A(z)A(z^{-1}) - B(z)B(z^{-1}) = \sum_{n=-N}^{N} (d_n - c_n) z^{-n}. \tag{15}$$

The polynomial $\Upsilon(z)$ can be represented as:

$$\Upsilon(z) = \sum_{n=0}^{N} \zeta_n z^{-n},$$

which includes the roots of $\Upsilon(z)\Upsilon(z^{-1})$ [the zeros or roots of the polynomial (15)] inside the unit circle. The output response of the zero-phase filter $G(z)$ can be represented as

$$X^s(z) = \frac{B(z)B(z^{-1})}{B(z)B(z^{-1}) + \Upsilon(z)\Upsilon(z^{-1})} Y(z), \tag{16}$$

where $X^s(z)$ is the zero-phase (smoothing) filter output. We assume that $G(z)$ is designed such that it passes the frequency components of x_k and removes the unwanted frequency components (i.e., η_k). Therefore, we could say that x_k^s is an estimate of x_k (i.e., $x_k^s \approx x_k$). In the best case, $x_k^s = x_k$. In the following, we show that the impulse response of the zero-phase filter $G(z)$ can be formed as an optimal smoothing Wiener filter for a random process obtained from an ARMA model driven by input white (innovation) noise in presence of a white or colored observation noise.

3.1. An equivalent smoothing Wiener filter for zero-phase IIR filters

The equivalent smoothing Wiener filter for zero-phase IIR filter, $G(z)$, is depicted in Fig. 2. To show it, we consider the Wiener smoothing filter that produces the minimum mean square error (MMSE) estimation of x [24,25]

$$G_W(z) = \frac{S_{xx}(z)}{S_{xx}(z) + S_{\eta\eta}(z)}, \tag{17}$$

where $S_{xx}(z)$ and $S_{\eta\eta}(z)$ are the power spectral density (PSD) of x_k and η_k, respectively. According to the process model, the

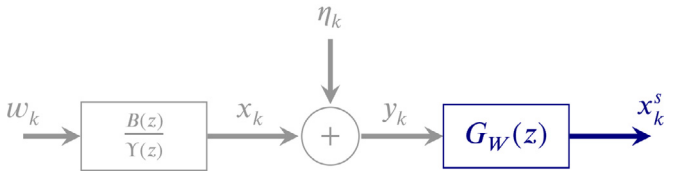

Fig. 2. The block diagram of smoothing Wiener filter for zero-phase IIR filters defined by (11) or (13), (14)) when $S_{\eta\eta}(z) = S_{ww}(z)$ or $\eta_k = w_k$.

PSD of the signal and process noise are related as $Sxx(z) = \frac{B(z)B(z^{-1})}{\Upsilon(z)\Upsilon(z^{-1})} s_{\eta\eta}(z)$. Using it in (17) and after some manipulation, (17) is simplified to

$$G_W(z) = \frac{B(z)B(z^{-1})}{B(z)B(z^{-1}) + \frac{S_{\eta\eta}(z)}{S_{ww}(z)}\Upsilon(z)\Upsilon(z^{-1})}. \tag{18}$$

Comparing (18) with (14), we conclude that they are equivalent if in Fig. 2, we set $S_{\eta\eta}(z) = S_{ww}(z)$ or $\eta_k = w_k$. In other word, $G(z)$ is a special case of the Wiener smoothing filter. Note that in Fig. 2, the desired signal is modeled as an ARMA process obtained by filtered the additive noise, w_k through the rational filter with transfer function $B(z)/\Upsilon(z)$, i.e., $x_k = B(z)/\Upsilon(z)w_k$ and the observed signal, y_k is the sum of an ARMA signal and a noise process, η_k:

$$\begin{cases} \frac{\Upsilon(z)}{B(z)} x_k = w_k \\ y_k = x_k + \eta_k \end{cases} \tag{19}$$

In a special case, when $S_{\eta\eta}(z) = S_{ww}(z)$ or $\eta_k = w_k$, (19) represents a linear state-space model of the zero-phase IIR filter (14). In general, Kalman filter/smoother can be used to estimate the signal of interest. The problem is that the state space model (19) cannot be used in the Kalman filter framework as the signal is described in the form of ARMA model. It must be expressed in the form of AR(1) model. To that end, in the following, an easy trick is proposed to modify the representation such that it is described by an AR(1) model. The following change of variable is suggested:

$$x_k = B(z)F_k$$

In this case, (19) is rewritten as

$$\begin{cases} \Upsilon(z)F_k = w_k \\ y_k = B(z)F_k + \eta_k \end{cases}.$$

It can be expressed in the following state-space form

$$\begin{cases} \boldsymbol{\xi}_k &= \boldsymbol{\Phi}\boldsymbol{\xi}_{k-1} + \boldsymbol{\sigma} w_k \\ y_k &= \boldsymbol{h}\boldsymbol{\xi}_k + \eta_k \end{cases}, \tag{20}$$

where $\boldsymbol{\xi}_k = [F_k, F_{k-1}, \ldots, F_{k-N}]^T$, $\boldsymbol{\sigma} = [1, 0, \ldots, 0]^T$, $\boldsymbol{h} = [b_0, b_1, \ldots, b_N]$ and

$$\boldsymbol{\Phi} = \begin{pmatrix} -\zeta_1 & -\zeta_2 & \ldots & -\zeta_N & 0 \\ 1 & 0 & \ldots & 0 & 0 \\ 0 & \ddots & \ddots & \vdots & \vdots \\ \vdots & \ddots & 1 & 0 & 0 \\ 0 & \ldots & 0 & 1 & 0 \end{pmatrix}.$$

The state of the system in (20), can be estimated using Kalman filter or smoother structure. Once an estimate of $\boldsymbol{\xi}_k$ is computed, an estimate of the desired signal is obtained by $x_k = \boldsymbol{h}\boldsymbol{\xi}_k$.

Note that the unwanted signal, f_k, and the desired signal, x_k, are on disjoint frequency ranges. This motivates us to modify the Wiener or Kalman filter model to improve the proposed approach.

Kalman filter-based Digital IIR Filter Design

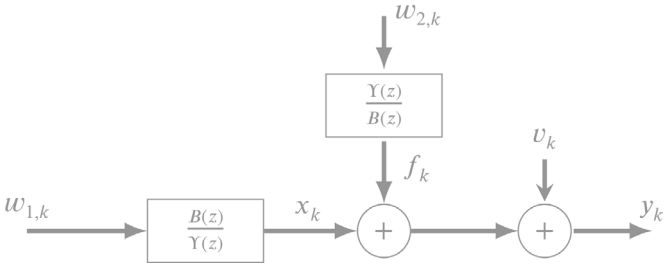

Fig. 3. An improved model for zero-phase IIR filters.

The idea is to model the signal f_k and estimate it using Kalman filter/smoother. In the following, we propose an improved model to compute the output response of digital IIR filters. In the new model, we represent f_k as an ARMA model and consider it as an extra state in the system model. The signals x_k and f_k are both considered as hidden state and estimated separately using Kalman filter/smoother.

3.2. Improved model

We propose the following model:

$$\begin{cases} \frac{\Upsilon(z)}{B(z)} x_k = w_{1,k} \\ \frac{B(z)}{\Upsilon(z)} f_k = w_{2,k} \\ y_k = x_k + f_k + v_k \end{cases}. \tag{21}$$

The block diagram of the improved model is shown in Fig. 3. The main advantage of the new model is that the observation noise is now a white Gaussian process. Therefore, the Kalman filter is an optimal estimator in MMSE sense to estimate the state of (21).

However, it must be represented in the form of AR(1) model. The following change of variables are suggested:

$$\begin{cases} x_k = B(z)F_{1,k} \\ f_k = \Upsilon(z)F_{2,k} \end{cases}$$

In this case, (21) is written as

$$\begin{cases} \Upsilon(z)F_{1,k} = w_{1,k} \\ B(z)F_{2,k} = w_{2,k} \\ y_k = B(z)F_{1,k} + \Upsilon(z)F_{2,k} + v_k \end{cases}$$

It can be expressed in the form of

$$\begin{cases} \boldsymbol{\xi}_k = \boldsymbol{\Phi}\boldsymbol{\xi}_{k-1} + \boldsymbol{\Sigma}\boldsymbol{w}_k \\ y_k = \boldsymbol{h}\boldsymbol{\xi}_k + v_k \end{cases}, \tag{22}$$

where $\boldsymbol{\xi}_k = [F_{1,k}, \ldots, F_{1,k-N}, F_{2,k}, \ldots, F_{2,k-N}]^T$, $\boldsymbol{h} = [\boldsymbol{h}_1, \boldsymbol{h}_2]$, $\boldsymbol{h}_1 = [b_0, b_1, \ldots, b_N]$, $\boldsymbol{h}_2 = [\zeta_0, \zeta_1, \ldots, \zeta_N]$, $\boldsymbol{w}_k = [w_k, w_k]^T$,

$$\boldsymbol{\Phi}=\begin{bmatrix}\boldsymbol{\Phi}_1 & \mathbf{0}\\ \mathbf{0} & \boldsymbol{\Phi}_2\end{bmatrix},\ \boldsymbol{\Phi}_1=\begin{pmatrix}-\zeta_1 & -\zeta_2 & \dots & -\zeta_N & 0\\ 1 & 0 & \dots & 0 & 0\\ 0 & \ddots & \ddots & \vdots & \vdots\\ \vdots & \ddots & 1 & 0 & 0\\ 0 & \dots & 0 & 1 & 0\end{pmatrix},$$

$$\boldsymbol{\Phi}_2=\begin{pmatrix}-b_1 & -b_2 & \dots & -b_N & 0\\ 1 & 0 & \dots & 0 & 0\\ 0 & \ddots & \ddots & \vdots & \vdots\\ \vdots & \ddots & 1 & 0 & 0\\ 0 & \dots & 0 & 1 & 0\end{pmatrix},$$

$$\boldsymbol{\Sigma}=\begin{pmatrix}1, \underbrace{0,\dots,0}_{N-\text{times}}, 0, \underbrace{0,\dots,0}_{N-\text{times}}\\ 0,\ 0,\dots,0,\ 1,\ 0,\dots,0\end{pmatrix}^T$$

The variance associated with the prediction $\hat{\boldsymbol{\xi}}_{k+1|k}$ of an unknown true value $\boldsymbol{\xi}_{k+1}$ is given by $\boldsymbol{P}_{k+1}^{-}=\boldsymbol{\Phi}_k\boldsymbol{P}_k^{+}\boldsymbol{\Phi}_k^T+\boldsymbol{\Sigma}_k^T\boldsymbol{Q}\boldsymbol{\Sigma}_k$, where $\boldsymbol{Q}\triangleq\mathbb{E}\{\boldsymbol{w}_k^T\boldsymbol{w}_k\}$. Note that the state $\boldsymbol{\xi}_k$ is estimated using Kalman filter/smoother. After estimating the hidden state $\boldsymbol{\xi}_k$, the desired signal, $x_k=F_{1,k}$, is computed by $x_k=[\boldsymbol{h}_1,\ \mathbf{0}]\boldsymbol{\xi}_k$, where $\mathbf{0}$ is a zero vector.

4. Example

In this section, the proposed approach is used to compute the output response of (zero-phase) low-pass (LP) and high-pass (HP) Butterworth filter using Kalman filter/smoother. The examples are borrowed from Selesnick et al. [19]. First, we present the Kalman filter formulation for LP and HP filters when the observation noise is a white Gaussian process. Then, the improved model is used to implement Kalman filter for output computation of Butterworth filter in the presence of both Gaussian and colored noise.

4.1. High-pass filter

Consider a Nth order zero-phase HP Butterworth filter described by Selesnick et al. [19, Eq. (49)]

$$G(z)=\frac{(-z+2-z^{-1})^N}{(-z+2-z^{-1})^N+\alpha^{2N}(z+2+z^{-1})^N}. \tag{23}$$

It is maximally-flat at $\omega=0$ and at the Nyquist frequency. The parameter α can be set so that the filter response has a specified cutoff frequency. To have a filter with a cutoff frequency ω_c, the value of α is obtained by setting the gain at cutoff frequency to 0.5, which gives

$$\alpha=\left[\frac{1-\cos\omega_c}{1+\cos\omega_c}\right]^{\frac{1}{2}}=\tan\frac{\omega_c}{2}. \tag{24}$$

It can be written as

$$G(z)=\frac{[(1-z^{-1})(1-z)]^N}{[(1-z^{-1})(1-z)]^N+\alpha^{2N}[(1+z^{-1})(1+z)]^N}, \tag{25}$$

where

$$\Upsilon(z)=\alpha^N(1+z^{-1})^N,\quad B(z)=(1-z^{-1})^N. \tag{26}$$

So, the linear state-space model corresponding to (23) can be represented as

$$\begin{cases}\alpha^N\frac{(1+z^{-1})^N}{(1-z^{-1})^N}x_k^{hp}=w_k\\ y_k=x_k^{hp}+\eta_k\end{cases}, \tag{27}$$

where x_k^{hp} stands for high-frequency component signal. Using the following change of variable

$$x_k^{hp}=\frac{1}{\alpha^N}(1-z^{-1})^N F_k=\sum_{i=0}^{N}\frac{1}{\alpha^N}(-1)^i\binom{N}{i}z^{-i}F_k,$$

Eq. (27) is represented in the form of (20), where $\binom{N}{i}$ is the binomial coefficient, $b_i=\frac{1}{\alpha^N}(-1)^i\binom{N}{i}$ and $\zeta_i=\binom{N}{i}$. Note that the digital Butterworth filter transform (23) is designed using bilinear transformation of the classical analog Butterworth filter. An alternative transfer function can be designed using step invariance method [10]. In Section Appendix A.1, we tackle the same problem of computing the output response of a HP Butterworth filter using Kalman filter when it is designed by step invariance.

4.2. Low-pass filter

A Nth order zero-phase LP Butterworth filter is described by Selesnick et al. [19, Eq. (50)]

$$G(z)=\frac{\alpha^{2N}(z+2+z^{-1})^N}{\alpha^{2N}(z+2+z^{-1})^N+(-z+2-z^{-1})^N}. \tag{28}$$

It can be written as

$$G(z)=\frac{\alpha^{2N}[(1+z^{-1})(1+z)]^N}{\alpha^{2N}[(1+z^{-1})(1+z)]^N+[(1-z^{-1})(1-z)]^N}, \tag{29}$$

where

$$\Upsilon(z)=(1-z^{-1})^N,\quad B(z)=\alpha^N(1+z^{-1})^N. \tag{30}$$

The equivalent smoothing Wiener filter for zero-phase LP Butterworth filter is depicted in Fig. 4. So, the linear state-space model corresponding to (28) can be represented as

$$\begin{cases}\frac{1}{\alpha^N}\frac{(1-z^{-1})^N}{(1+z^{-1})^N}x_k^{lp}=w_k\\ y_k=x_k^{lp}+\eta_k\end{cases} \tag{31}$$

where x_k^{lp} stands for low-frequency component signal. Using the following change of variable

$$x_k^{lp}=\alpha^N(1+z^{-1})^N F_k=\sum_{i=0}^{N}\alpha^N\binom{N}{i}z^{-i}F_k,$$

Eq. (31) is represented in the form of (20), where $b_i=\alpha^N\binom{N}{i}$ and $\zeta_i=(-1)^i\binom{N}{i}$. In Section Appendix A.2, we tackle the same problem of formulating the output response computation of a LP Butterworth filter using Kalman filter when it is designed by step invariance.

4.3. Improved low/high-pass filter model

The previous HP and LP filters are optimal if the observation noise is a white Gaussian process. In the presence of colored observation noise, the optimal model is defined as

$$\begin{cases}\frac{1}{\alpha^N}\frac{(1-z^{-1})^N}{(1+z^{-1})^N}x_k^{lp}=w_{1,k}\\ \alpha^N\frac{(1+z^{-1})^N}{(1-z^{-1})^N}x_k^{hp}=w_{2,k}\\ y_k=x_k^{lp}+x_k^{hp}+v_k\end{cases}. \tag{32}$$

Using the change of variables

$$\begin{cases}x_k^{lp}=\alpha^N(1+z^{-1})^N F_{1,k}\\ x_k^{hp}=\frac{1}{\alpha^N}(1-z^{-1})^N F_{2,k}\end{cases},$$

Eq. (32) is written in the form of (22), where $b_i=\binom{N}{i}$ and $\zeta_i=(-1)^i\binom{N}{i}$, $\boldsymbol{h}_1=\alpha^N[b_0,\ b_1,\dots,\ b_N]$ and $\boldsymbol{h}_2=1/\alpha^N[\zeta_0,\ \zeta_1,\dots,\ \zeta_N]$.

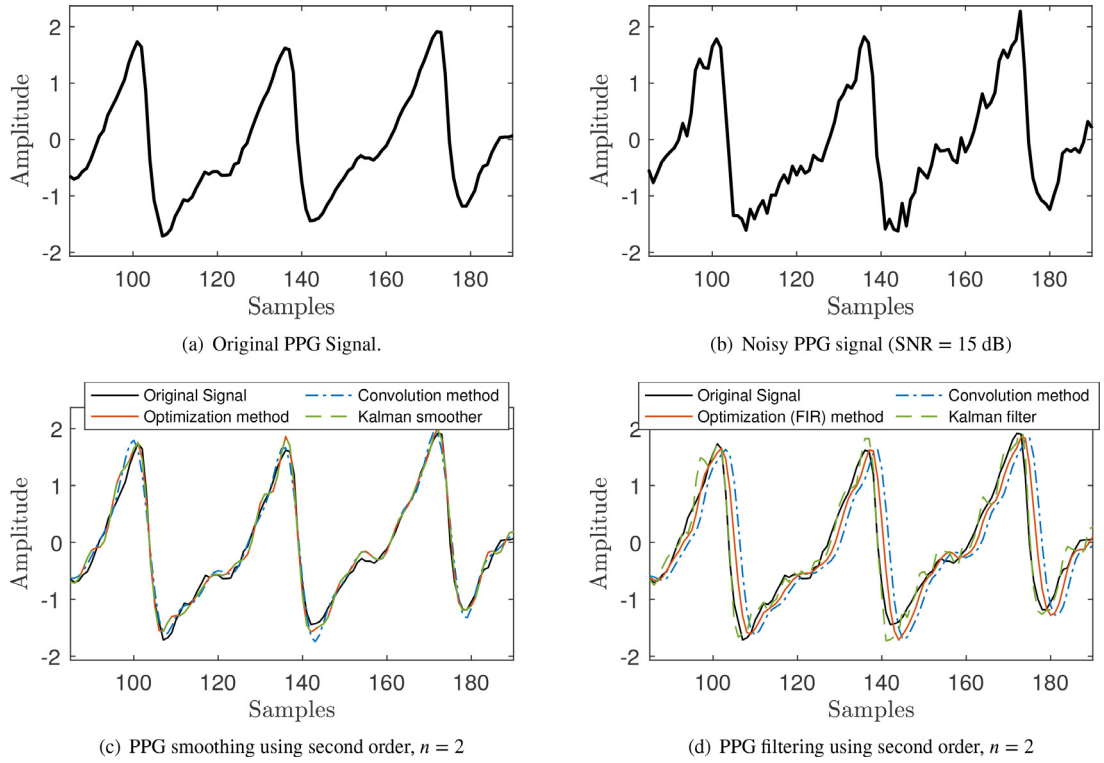

(a) Original PPG Signal.

(b) Noisy PPG signal (SNR = 15 dB)

(c) PPG smoothing using second order, $n = 2$

(d) PPG filtering using second order, $n = 2$

Fig. 4. An equivalent smoothing Wiener filter for zero-phase low-pass Butterworth filter when $S_{\eta\eta}(z) = S_{ww}(z)$ or $\eta_k = w_k$.

After estimating the hidden state $\boldsymbol{\xi}$ using Kalman filter/smoother, the desired signal, $x_k^{lp} = F_{1,k}$, is computed by $x_k^{lp} = [\boldsymbol{h}_1,\ \mathbf{0}]\boldsymbol{\xi}_k$. When the objective is to design a HP filter, the desired signal, $x_k^{hp} = F_{2,k}$, is computed by $x_k^{hp} = [\mathbf{0},\ \boldsymbol{h}_2]\boldsymbol{\xi}_k$.

5. Accuracy comparison

In this section, Photoplethysmograph (PPG) signal filtering and smoothing are considered for comparing the accuracy of the three approaches based output computation of zero-phase LP Butterworth filter: traditional output computation (i.e., by convolution of the input signal with the Butterworth impulse response), the optimization approach based output computation of (zero-phase) Butterworth filter [10] and the Kalman filter/smoother based output estimation of Butterworth filter. PPG is one of the most widely used method to measure cardiovascular status due to its simplicity in recording. It is usually measured at body extremities, such as fingers, ears, and wrists. It is considered minimally invasive and cost effective procedure which provides clinical and physiological information about the cardiovascular system. The main problem is that it is usually corrupted with unwanted interference, generally referred to as noise or undesired artifacts. This limitation might mask the useful information. A common approach to remove the undesired signal is to use a digital IIR filter. In this paper, we use a digital LP Butterworth filter.

See Fig. 5(b), for an example, where the plotted curve denotes the noisy data obtained by sampling the original PPG signal plotted in Fig. 5(a). The observed data is the result of contaminating the true PPG signal by a Gaussian random noise SNR = 15 dB. The original PPG is a specific case from the Real-World PPG dataset [21]. The dataset contains PPG signals from 35 healthy persons, with 50 to 60 PPG signal for each one. Each PPG signal contains 300 samples (6 s recording) with 50 sample/second sampling rate. The output response of zero-phase LP Butterworth filter were computed using the traditional convolution method following by forward-backward filtering (i.e., using the Matlab command *filtfilt*), optimization approach [10] and the Kalman smoother. To quantify the performance of the methods, we employed noise to signal ratio (NSR), i.e., the classical ratio between the power of the reconstruction error and the power of the original signal, given by Kheirati

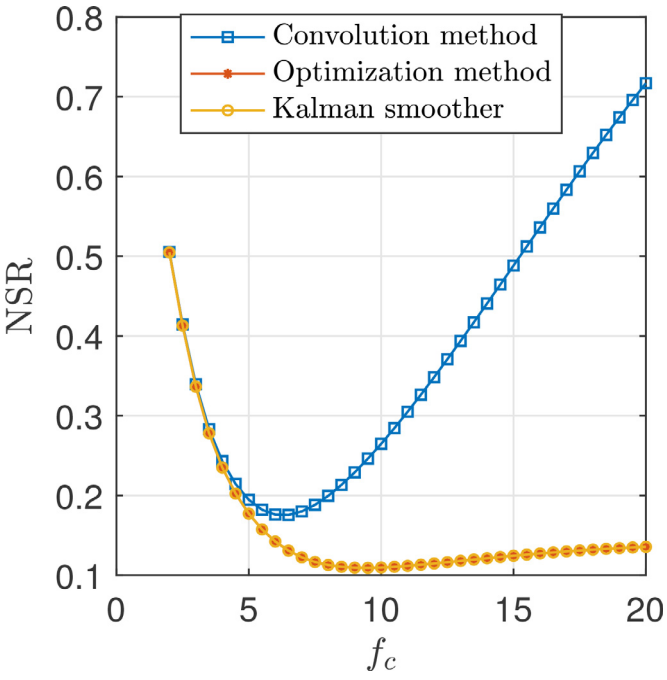

Fig. 5. The output result of second order (zero-phase) LP Butterworth filter using conventional convolution approach, optimization method and Kalman filter/smoother method. (a) Original PPG signal (b) noisy PPG signal (c) the output of zero-phase LP Butterworth filter (d) the output of causal LP Butterworth filter.

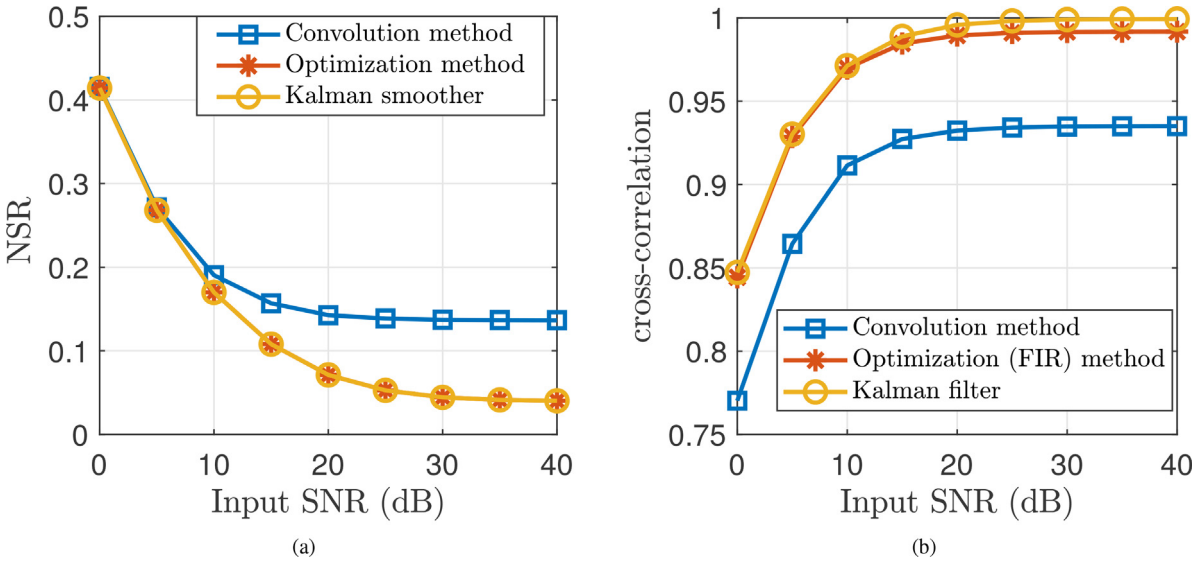

Fig. 6. The variations of NSR as a function of cutoff frequency.

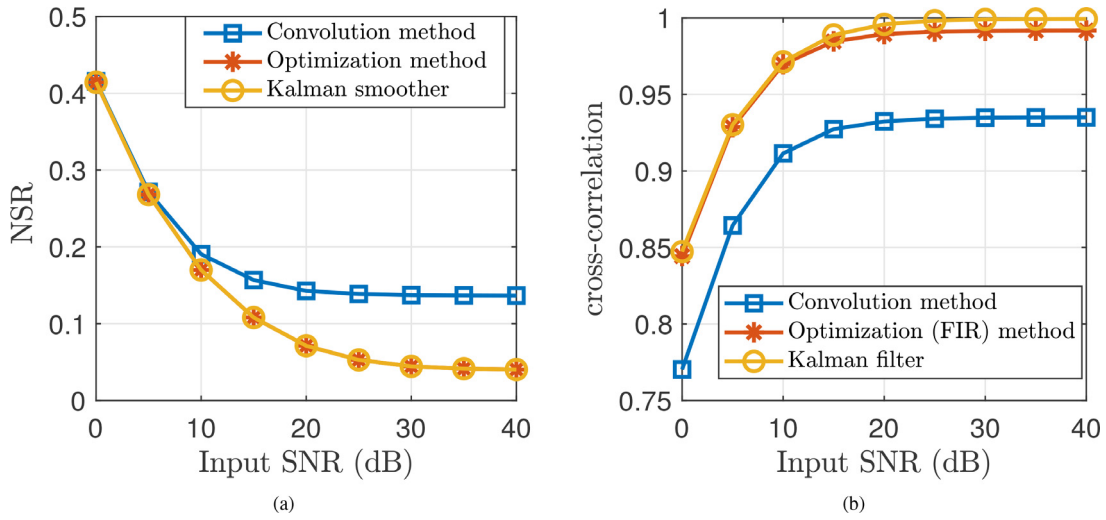

Fig. 7. Comparing three output computation approaches based Butterworth filter design for PPG signal filtering and smoothing. (a) The mean values of NSR for signal reconstruction obtained by zero-phase Butterworth filter as a functions of input SNR. (b) The mean values of Cross-correlation for signal reconstruction obtained by Butterworth filter as a functions of input SNR.

Roonizi [3]

$$\mathrm{NSR} = \sqrt{\frac{\sum_k \left(x_k - \hat{x}_k\right)^2}{\sum_k x_k^2}},$$

where x_k is the true PPG signal and $\hat{x}_k$ is the filter output. In Fig. 5(c), the results of PPG smoothing using zero-phase Butterworth filter designed by the mentioned approaches are shown. The cutoff frequency was chosen such that for each method the NSR was minimized in signal reconstruction when f_c changes from 2 to 20 Hz. The variations of NSR as a function of cutoff frequency for this example is plotted in Fig. 6. The output response of zero-phase Butterworth filter when implemented by Kalman smoother and Wiener smoother are equivalent (i.e., the NSR is equal for both methods). For $f_c \leq 3.5$ Hz, the accuracy of zero-phase Butterworth filter when implemented by traditional forward-backward filtering is close to that of implemented by Kalman smoother or Wiener smoother. However, as we increase the value of cutoff frequency form 3.5 to 20, the accuracy of the conventional forward-backward filtering is less than the accuracy of Kalman or Wiener smoother. The reason is that when the output response of Butterworth filter is computed using Wiener or Kalman smoother, the filter is robust to white Gaussian noise.

The cutoff frequency that minimizes the NSR for Kalman and Wiener smoother is $f_c = 10$ Hz, while it is $f_c = 6$ Hz for conventional implementation. After that we see that the accuracy of zero-phase Butterworth filter is dramatically decreased for the traditional implementation while it does not happen for Wiener or Kalman smoother. In other words, the zero-phase filter is less sensitive to cutoff frequency when its output is computed using Kalman or Wiener smoother. The cutoff frequency corresponds to the minimum value of the curve (the place where the graph has a vertex at its lowest point) was then chosen as the optimal value of cutoff frequency for each method. The result of PPG reconstruction using each approach for the optimal value of cutoff frequency is plotted in Fig. 5(c). It is also seen from Fig. 5(c) that the output results of the zero-phase Butterworth filter computed by optimization problem (or Wiener smoothing filter) and Kalman smoother are the same while they are slightly different from output response of zero-phase Butterworth filter computed by traditional convolution method. In Fig. 5(d), we show the result of PPG filtering using

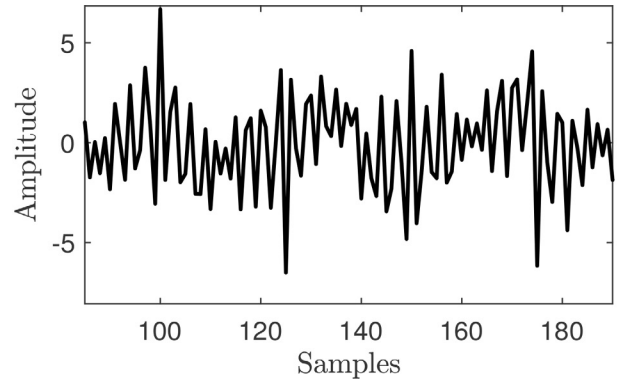

(a) Noisy PPG signal

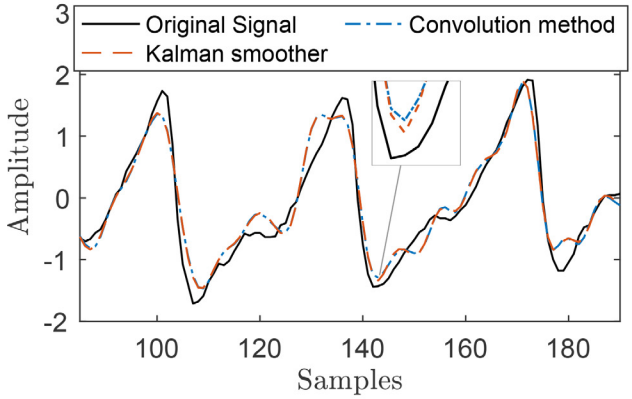

(b) PPG smoothing using second order zero-phase Butterworth filter

Fig. 8. The output result of second order zero-phase LP Butterworth filter using conventional convolution approach (NSR = 0.31) and Kalman smoother method (NSR = 0.28). (a) noisy PPG signal contaminated by a high-frequency noise (b) Output response of zero-phase LP Butterworth filter.

Butterworth filter implemented by traditional causal filter design (i.e., using the Matlab command *filter*), FIR Butterworth filter design proposed in Kheirati Roonizi and Jutten [10] and Kalman filter. The traditional convolution method imply time-shifts varying according to the frequency while the Kalman filter does not. Finally, we compared the three zero-phase output computation approaches using the whole dataset. To this purpose, we added noises with varying power to the original PPG signals. The signal-to-noise ratio (SNR) was modulated from 0 to 40 dB. Then the PPG signal was estimated from the noisy PPGs. The mean values of NSR for signal reconstruction obtained by three methods as a function of SNR is shown in Fig. 7(a). It is seen that the output computation based optimization problem and Kalman smoother are the same while they are better than traditional convolution method. We also compared those methods based filter output computation. Since the traditional convolution method induces delay, we compared them using cross-correlation. The results of comparison using cross-correlation are reported in Fig. 7(b). In the best case of signal reconstruction, the cross-correlation should be close to 1. The result of Fig. 7(b) shows that the Kalman filter based method outperforms traditional convolution method in computing the output of Butterworth filter.

In the above experiment, we showed the merit of the proposed Kalman filter-based output computation of digital LP Butterworth filter for filtering out the white Gaussian noise. In the next experiment, we considered the problem of colored noise filtering using Butterworth filter. To this end, the improved approach was used to implement the Butterworth filter. See Fig. 8(a), for an example, where the plotted curve denotes the noisy data obtained by sampling the same PPG signal in Fig. 5(a). The observed data is the result of contaminating the true PPG signal by a high-frequency components signal and a white noise. In Fig. 8(b), the results of PPG smoothing using zero-phase Butterworth filter designed by the mentioned approaches are shown. The cutoff frequency was again chosen such that NSR was minimized in signal reconstruction. The value of NSR for each method is also reported for quantitative comparison which indicates that the Kalman smoother outperforms traditional convolution method based output computation of Butterworth filter. The quantitative comparison for signal reconstruction for whole dataset using (zero-phase) Butterworth filter obtained by convolution method and Kalman filter is shown in Fig. 9. The Kalman filter/smoother outperforms traditional convolution method based output computation of (zero-phase) Butterworth filter when the noise comprises a high-frequency signal and a white noise.

6. Summary

This paper proposes an optimal Kalman filter/smoother framework to find the output response of (zero-phase) digital IIR filters. It shows that every digital IIR filter can be viewed as an optimal

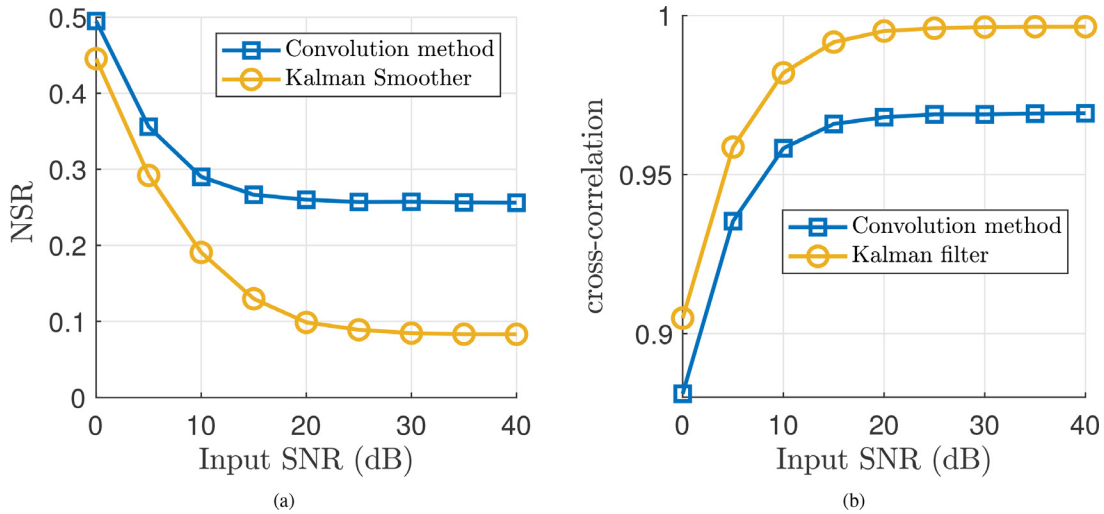

(a) (b)

Fig. 9. Comparing the approaches based output computation of (zero-phase) Butterworth filter for PPG signal filtering and smoothing when the noise comprises a high-frequency signal and a white noise.

smoothing Wiener filter. Then based on the fact that the formulations of the optimum filter by Wiener and Kalman are equivalent in steady state, the paper presents a Kalman filter framework to find the optimal output response of digital IIR filters in minimum mean square error sense. As an example, the output response of (zero-phase) digital Butterworth filter is computed using Kalman filter/smoother and compared with the traditional convolution method output computation.

The proposed approach has several advantages in comparison with the traditional convolutional approach for computing the output response of digital IIR filters. Using it, the digital IIR filters can be used for optimal reconstruction of the signal when the unwanted signal contains white Gaussian noise as it also estimates the noise while filtering. The proposed theory can also be used for the combination of zero-phase digital IIR filters with other signal processing algorithms for more complicated signal reconstruction models. In the future, we will extend it for reconstructing signals that comprise of a band-limited component and other signal models. For instance, we will use it for electrocardiogram (ECG) signal processing. In this case, the recorded ECG signal comprises an ECG signal which can be modeled as a sum of Gaussian functions [4,6,7], power-line interference (PLI) which can be detected using a narrow-band band-pass filter Kheirati Roonizi [3, eq. 56], a baseline wander (BW) signal which can be detected by a low-pass filter and a random noise. To design a simultaneous Gaussian signal, low-pass and band-pass signal detection algorithm, one can combine the dynamical model of Gaussian signal and zero-phase digital IIR filters to track the signals of interest in the framework of Kalman filter/smoother.

Declaration of Competing Interest

Author declare that he does has no conflict of interest.

Data availability

The data is described in the paper.

Acknowledgment

Part of this research was supported by the MUSA – Multilayered Urban Sustainability Action – project, funded by the European Union – NextGenerationEU, under the National Recovery and Resilience Plan (NRRP) Mission 4 Component 2 Investment Line 1.5: Strenghtening of research structures and creation of R&D "innovation ecosystems", set up of "territorial leaders in R&D"

Appendix A

In this section, we tackle the same problem (i.e., Kalman filter formulation of zero-phase Butterworth filter) using step invariance.

A1. Zero-phase HP Butterworth filter using step invariance

The Nth order zero-phase digital HP Butterworth filter, using step invariance, is described by Kheirati Roonizi and Jutten [10]

$$G(z) = \frac{(-z+2-z^{-1})^N}{(-z+2-z^{-1})^N + \alpha^{2N}}. \tag{33}$$

In this case, $B(z) = (1-z^{-1})^N$, $\Upsilon(z) = \alpha^N$ and $\alpha = 1/(2\sin\omega_c/2)$. Comparing (33) and (25), the only difference is that the coefficients of $\Upsilon(z)$ in (25) is $\zeta_i = \binom{N}{i}$ while the coefficients of $\Upsilon(z)$ in (33) is

$$\zeta_i = \begin{cases} \alpha^N & i = 0 \\ 0 & i \neq 0 \end{cases}$$

The problem is that $\Upsilon(z)$ is constant in (33). In this case, we might multiply its nominator and denominator by $1-z^{-1}$. In this case, (33) is written as

$$G(z) = \frac{(1-z^{-1})(-z+2-z^{-1})^N}{(1-z^{-1})(-z+2-z^{-1})^N + \alpha^{2N}(1-z^{-1})}. \tag{34}$$

The Kalman filter implementation of zero-phase digital HP Butterworth filter using step invariance is straightforward.

A2. Zero-phase LP Butterworth filter using step invariance

Similarly, the Nth order zero-phase digital LP Butterworth filter transform using step invariance is described by Kheirati Roonizi and Jutten [10]

$$G(z) = \frac{\alpha^{2N}}{\alpha^{2N} + (-z+2-z^{-1})^N}. \tag{35}$$

In that case, $B(z) = \alpha^N$, $\Upsilon(z) = (1-z^{-1})^N$. The Kalman filter implementation of zero-phase digital LP Butterworth filter using step invariance is straightforward. Comparing (35) and (29), the only difference is that the coefficients of $B(z)$ in (29) is $b_i = \binom{N}{i}$ while the coefficients of $B(z)$ in (35) is

$$b_i = \begin{cases} \alpha^N & i = 0 \\ 0 & i \neq 0 \end{cases}$$

References

[1] A. Jiang, H.K. Kwan, Minimax design of IIR digital filters using iterative SOCP, IEEE Trans. Circuits Syst. I 57 (6) (2010) 1326–1337.
[2] R.E. Kalman, A new approach to linear filtering and prediction problems, J. Basic Eng. 82 (1960) 35–45.
[3] A. Kheirati Roonizi, A new approach to ARMAX signals smoothing: application to variable-Q ARMA filter design, IEEE Trans. Signal Process 67 (17) (2019) 4535–4544.
[4] A. Kheirati Roonizi, A new approach to gaussian signal smoothing: application to ECG components separation, IEEE Signal Process. Lett. 27 (2020) 1924–1928, doi:10.1109/LSP.2020.3031501.
[5] A. Kheirati Roonizi, ℓ_2 and ℓ_1 trend filtering: a Kalman filter approach, IEEE Signal Process. Mag. 38 (6) (2021) 137–145.
[6] E. Kheirati Roonizi, A new algorithm for fitting a Gaussian function riding on the polynomial background, Signal Process. Lett., IEEE 20 (11) (2013) 1062–1065.
[7] E. Kheirati Roonizi, R. Sassi, A signal decomposition model-based Bayesian framework for ECG components separation, IEEE Trans. Signal Process. 64 (3) (2016) 665–674, doi:10.1109/TSP.2015.2489598.
[8] A. Kheirati Roonizi, C. Jutten, Improved smoothness priors using bilinear transform, Signal Process. 169 (2020) 107381.
[9] A. Kheirati Roonizi, C. Jutten, Band-stop smoothing filter design, IEEE. Trans. Signal Process. 69 (2021) 1797–1810, doi:10.1109/TSP.2021.3060619.
[10] A. Kheirati Roonizi, C. Jutten, Forward-backward filtering and penalized least--squares optimization: a unified framework, Signal Process. 178 (2021) 107796.
[11] X. Lai, Z. Lin, Minimax design of IIR digital filters using a sequential constrained least-squares method, IEEE Trans. Signal Process 58 (7) (2010) 3901–3906.
[12] C.-L. Liu, S.-C. Pei, Closed-form output response of discrete-time linear time-invariant systems using intermediate auxiliary functions, IEEE Signal Process. Mag. 37 (5) (2020) 140–145, doi:10.1109/MSP.2020.3002484.
[13] A. Oppenheim, R. Schafer, Discrete-Time Signal Processing, Pearson Education, 2011.
[14] T.W. Parks, C.S. Burrus, Digital Filter Design, Wiley-Interscience, USA, 1987.
[15] W. Press, B. Flannery, S. Teukolsky, W. Vetterling, Numerical Recipes, The Art of Scientific computing, Cambridge University Press, New York, NY, 1986.
[16] B. Psenicka, F. Garcia-Ugalde, J. Savage, S. Herrera-Garcia, V. Davidek, Design of state digital filters, IEEE Trans. Signal Process. 46 (9) (1998) 2544–2549, doi:10.1109/78.709543.
[17] H. Qi, Z.G. Feng, K.F.C. Yiu, S. Nordholm, Optimal design of IIR filters via the partial fraction decomposition method, IEEE Trans. Circuits Syst. II 66 (8) (2019) 1461–1465.
[18] L. Rabiner, N. Graham, H. Helms, Linear programming design of IIR digital filters with arbitrary magnitude function, IEEE Trans. Acoust., Speech, Signal Process. 22 (4) (1974) 117–123.
[19] I.W. Selesnick, H.L. Graber, D.S. Pfeil, R.L. Barbour, Simultaneous low-pass filtering and total variation denoising, IEEE Trans. Signal Process 62 (5) (2014) 1109–1124, doi:10.1109/TSP.2014.2298836.
[20] B. Shahrrava, Closed-form impulse responses of linear time-invariant systems: a unifying approach, IEEE Signal Process. Mag. 35 (4) (2018) 126–132, doi:10.1109/MSP.2018.2810300.

[21] A. Siam, F. Abd El-Samie, A. Abu Elazm, N. El-Bahnasawy, G. Elbanby, Real-world PPG dataset, Mendeley Data V1 (2019) doi:10.17632/yynb8t9x3d.1.
[22] D. Simon, Optimal State Estimation: Kalman, H Infinity, and Nonlinear Approaches, Wiley, 2006.
[23] J.O. Smith, Introduction to Digital Filters with Audio Applications, W3K Publishing, 2007.
[24] H. Van Trees, Detection, Estimation, and Modulation Theory, Part I: Detection, Estimation, and Linear Modulation Theory, Wiley, 2004.
[25] N. Wiener, Extrapolation, Interpolation, and Smoothing of Stationary Time Series : With Engineering Applications, Technology Press of the Massachusetts Institute of Technology, London, 1949.